JOURNAL OF Applied Polymer SCIENCE

Special Issue: Bio-based Packaging

Guest Editors: José M. Lagarón, Amparo López-Rubio, and María José Fabra
Institute of Agrochemistry and Food Technology of the Spanish Council for Scientific Research

EDITORIAL

REVIEWS

RESEARCH ARTICLES

JOURNAL OF Applied Polymer SCIENCE

Special Issue: Bio-based Packaging

Guest Editors: José M. Lagarón, Amparo López-Rubio, and María José Fabra
Institute of Agrochemistry and Food Technology of the Spanish Council for Scientific Research

Impact of fermentation residues on the thermal, structural, and rheological properties of polyhydroxy(butyrate-*co*-valerate) produced from cheese whey and olive oil mill wastewater
L. Hilliou, D. Machado, C. S. S. Oliveira, A. R. Gouveia, M. A. M. Reis, S. Campanari, M. Villano and M. Majone, *J. Appl. Polym. Sci.* 2015, DOI: 10.1002/app.42818

Synergistic effect of lactic acid oligomers and laminar graphene sheets on the barrier properties of polylactide nanocomposites obtained by the in situ polymerization pre-incorporation method
J. Ambrosio-Martín, A. López-Rubio, M. J. Fabra, M. A. López-Manchado, A. Sorrentino, G. Gorrasi and J. M. Lagarón, *J. Appl. Polym. Sci.* 2015, DOI: 10.1002/app.42661

Antibacterial poly(lactic acid) (PLA) films grafted with electrospun PLA/allyl isothiocyanate fibers for food packaging
H. H. Kara, F. Xiao, M. Sarker, T. Z. Jin, A. M. M. Sousa, C.-K. Liu, P. M. Tomasula and L. Liu, *J. Appl. Polym. Sci.* 2015, DOI: 10.1002/app.42475

Poly(L-lactide)/ZnO nanocomposites as efficient UV-shielding coatings for packaging applications
E. Lizundia, L. Ruiz-Rubio, J. L. Vilas and L. M. León, *J. Appl. Polym. Sci.* 2015, DOI: 10.1002/app.42426

Effect of electron beam irradiation on the properties of polylactic acid/montmorillonite nanocomposites for food packaging applications
M. Salvatore, A. Marra, D. Duraccio, S. Shayanfar, S. D. Pillai, S. Cimmino and C. Silvestre, *J. Appl. Polym. Sci.* 2015, DOI: 10.1002/app.42219

Preparation and characterization of linear and star-shaped poly L-lactide blends
M. B. Khajeheian and A. Rosling, *J. Appl. Polym. Sci.* 2015, DOI: 10.1002/app.42231

Mechanical properties of biodegradable polylactide/poly(ether-block-amide)/thermoplastic starch blends: Effect of the crosslinking of starch
L. Zhou, G. Zhao and W. Jiang, *J. Appl. Polym. Sci.* 2015, DOI: 10.1002/app.42297

Interaction and quantification of thymol in active PLA-based materials containing natural fibers
I. S. M. A. Tawakkal, M. J. Cran and S. W. Bigger, *J. Appl. Polym. Sci.* 2015, DOI: 10.1002/app.42160

Graphene-modified poly(lactic acid) for packaging: Material formulation, processing, and performance
M. Barletta, M. Puopolo, V. Tagliaferri and S. Vesco, *J. Appl. Polym. Sci.* 2015, DOI: 10.1002/app.42252

Edible films based on chia flour: Development and characterization
M. Dick, C. H. Pagno, T. M. H. Costa, A. Gomaa, M. Subirade, A. De O. Rios and S. H. Flóres, *J. Appl. Polym. Sci.* 2015, DOI: 10.1002/app.42455

Influence of citric acid on the properties and stability of starch-polycaprolactone based films
R. Ortega-Toro, S. Collazo-Bigliardi, P. Talens and A. Chiralt, *J. Appl. Polym. Sci.* 2015, DOI: 10.1002/app.42220

Bionanocomposites based on polysaccharides and fibrous clays for packaging applications
A. C. S. Alcântara, M. Darder, P. Aranda, A. Ayral and E. Ruiz-Hitzky, *J. Appl. Polym. Sci.* 2015, DOI: 10.1002/app.42362

Hybrid carrageenan-based formulations for edible film preparation: Benchmarking with kappa carrageenan
F. D. S. Larotonda, M. D. Torres, M. P. Gonçalves, A. M. Sereno and L. Hilliou, *J. Appl. Polym. Sci.* 2015, DOI: 10.1002/app.42263

JOURNAL OF Applied Polymer SCIENCE

Special Issue: Bio-based Packaging

Guest Editors: José M. Lagarón, Amparo López-Rubio, and María José Fabra
Institute of Agrochemistry and Food Technology of the Spanish Council for Scientific Research

Structural and mechanical properties of clay nanocomposite foams based on cellulose for the food packaging industry
S. Ahmadzadeh, J. Keramat, A. Nasirpour, N. Hamdami, T. Behzad, L. Aranda, M. Vilasi and S. Desobry, *J. Appl. Polym. Sci.* 2015, DOI: 10.1002/app.42079

Mechanically strong nanocomposite films based on highly filled carboxymethyl cellulose with graphene oxide
M. El Achaby, N. El Miri, A. Snik, M. Zahouily, K. Abdelouahdi, A. Fihri, A. Barakat and A. Solhy, *J. Appl. Polym. Sci.* 2015, DOI: 10.1002/app.42356

Production and characterization of microfibrillated cellulose-reinforced thermoplastic starch composites
L. Lendvai, J. Karger-Kocsis, Á. Kmetty and S. X. Drakopoulos, *J. Appl. Polym. Sci.* 2015, DOI: 10.1002/app.42397

Development of bioplastics based on agricultural side-stream products: Film extrusion of *Crambe abyssinica*/wheat gluten blends for packaging purposes
H. Rasel, T. Johansson, M. Gällstedt, W. Newson, E. Johansson and M. Hedenqvist, *J. Appl. Polym. Sci.* 2015, DOI: 10.1002/app.42442

Influence of plasticizers on the mechanical and barrier properties of cast biopolymer films
V. Jost and C. Stramm, *J. Appl. Polym. Sci.* 2015, DOI: 10.1002/app.42513

The effect of oxidized ferulic acid on physicochemical properties of bitter vetch (*Vicia ervilia*) protein-based films
A. Arabestani, M. Kadivar, M. Shahedi, S. A. H. Goli and R. Porta, *J. Appl. Polym. Sci.* 2015, DOI: 10.1002/app.42894

Effect of hydrochloric acid on the properties of biodegradable packaging materials of carboxymethylcellulose/poly(vinyl alcohol) blends
M. D. H. Rashid, M. D. S. Rahaman, S. E. Kabir and M. A. Khan, *J. Appl. Polym. Sci.* 2015, DOI: 10.1002/app.42870

Journal of Applied Polymer Science

Characterization of polyhydroxyalkanoate blends incorporating unpurified biosustainably produced poly(3-hydroxybutyrate-*co*-3-hydroxyvalerate)

Antonio Martínez-Abad,[1] Luis Cabedo,[2] Catarina S. S. Oliveira,[3] Loic Hilliou,[4] Maria Reis,[3] José María Lagarón[1]

[1]Novel Materials and Nanotechnology Group, IATA, CSIC, Avda. Agustín Escardino 7, 46980, Burjassot, Spain
[2]Polymers and Advanced Materials Group (PIMA), Universitat Jaume I, 12071, Castellón, Spain
[3]UCIBIO, REQUIMTE, Departamento de Química, Faculdade de Ciências e Tecnologia, Universidade Nova de Lisboa, 2829-516, Caparica, Portugal
[4]Institute for Polymers and Composites/I3N, University of Minho, 4800-058 Guimarães, Portugal
Correspondence to: J. M. Lagarón (E-mail: lagaron@iata.csic.es)

ABSTRACT: Poly(3-hydroxybutyrate-*co*-3-hydroxyvalerate) (PHBV) produced by mixed bacterial cultures derived from a cheese whey (CW) industrial by-product (unpurified PHBV; u-PHBV) was incorporated into commercial PHBV without previous purification or isolation processes. The presence of certain impurities was evident as investigated by scanning electron microscopy. The crystallinity of the polymer fraction was decreased by about 3% compared to the commercial PHBV. The onset of thermal degradation was not substantially affected by the incorporation of the u-PHBV fraction. A higher flexibility and elongation at break was mostly attributed to the increased contents in 3-hydroxyvalerate in the blends with increasing u-PHBV content. Water and D-limonene vapor permeability were not affected up to u-PHBV contents of 15 wt %. This study puts forth the potential use of unpurified PHBV obtained from mixed microbial cultures and grown from industrial by-products as a cost-effective additive to develop more affordable and waste valorized packaging articles. © 2015 Wiley Periodicals, Inc. J. Appl. Polym. Sci. **2016**, *133*, 42633.

KEYWORDS: biopolymers and renewable polymers; blends; composites

Received 3 March 2015; accepted 22 June 2015
DOI: 10.1002/app.42633

INTRODUCTION

Polyhydroxyalkanoates (PHA's) are a family of naturally occurring storage biopolyesters synthesized by more than 300 species of Gram-positive and Gram-negative bacteria.[1] Among the various biodegradable polymers, PHA's provide a good alternative to fossil-fuel based plastics as they possess thermoplastic properties similar to conventional polyolefins, such as polypropylene, with the advantage of being 100% biodegradable, compostable and produced from renewable resources.[2–5] In the areas of food and cosmetic packaging, PHA's are already commercialized as cosmetic containers, shampoo bottles, covers, milk cartons and films, moisture barriers in nappies and sanitary towels, pens and combs, among others (reviewed by Ref. 6).

The excessive brittleness of hydroxybutyrate homopolymers (Polyhydroxybutyrate; PHB) can be surmounted by enhancing the synthesis of poly(3-hydroxybutyrate-*co*-3-hydroxyvalerate (PHBV) heteropolymers. It has been reported that increasing valerate content in PHBV results in higher flexibility, strength, elongation at break, and a lower melting temperature, which may widen the thermal processing window of these PHAs.[7]

Production of PHA's, however, involves fermentation, isolation, and purification processes, which imply higher production costs as compared to polyolefins. The production of PHBVs additionally involves the addition of relatively high concentrations of propionate, which can be detrimental. Therefore, much efforts and improvements have been developed to reduce the costs of the fermentation and downstream processes.[4,8] As an example, the use of open mixed cultures avoids the need for sterility in the reactor and allows the use of low cost agricultural or industrial waste feedstock in the production of PHA's.[4,9] Gurieff and Lant[10] performed a lifecycle assessment and financial analysis and proved that PHA production by mixed cultures from renewable resources is financially and environmentally attractive. Moreover, it is a greener alternative to the pure culture processes since less CO_2 is produced.[10] In a previous work, PHAs with different valerate content were produced by mixed

microbial cultures using a three-stage process and the effect of a feedstock shift, mimicking a seasonal feedstock scenario, was assessed using cheese whey (CW) and sugar cane molasses (SCM) as model feedstocks.[11] In that study, a relatively high productivity and purity of the PHBV was achieved using cheese whey. Cheese whey is an industrial by-product, whose potential due to high contents in proteins and sugars is mostly not fully valorized at present. If the use of mixed bacterial cultures allows a more efficient transformation of a heterogeneous mixture of nutrients into the desired product, relatively expensive isolation, and purification processes, typically involving solvent extraction, supercritical fluid extraction, hydrogen peroxide treatments, and other purification methods,[8] might be avoided or substantially reduced. Thus, the overall biosustainability of the process would be notably improved, both from the facts of using an industrial by-product easily available and from the absence of expensive and energy consuming purification processes to obtain the PHBV. Nevertheless, the absence of isolation and purification processes implies that a certain content of residual organic matter from the fermentation process will be present in the polymer matrix and might affect the physico-chemical properties of the final material, such as melt stability, tensile properties, etc.

In the present article, different amounts of a pilot-plant produced, unpurified PHBV (u-PHBV), obtained from a bacterial mixed culture grown using a cheese whey industrial by-product, were mixed with commercial PHBV by direct melt-compounding. The blends were characterized on their composition, morphology, and crystallinity, as well as on their thermal, mechanical, and barrier properties.

EXPERIMENTAL

Obtention of u-PHBV and PHBV Blends

The u-PHBV was produced from sweet cheese whey (supplied by a Portuguese cheese factory – Bel Portugal, Fábrica da Ribeira Grande), in a three-stage process comprising: (1) acidogenic fermentation of the cheese whey (CW), where the sugars present in the cheese whey were biologically converted to organic acids (HOrgs), which are the precursors for PHA; (2) selection of an efficient PHA-accumulating mixed microbial culture under feast and famine regime; and (3) PHA production where the selected PHA-accumulating culture was fed with the organic acids rich stream resultant from the acidogenic fermentation of cheese whey, until the cells reached maximum PHA storage content.

The acidogenic fermentation carried out in a continuous anaerobic membrane bioreactor (AnMBR), consisting of a 10 L reactor (BioStat® B plus, Sartorius) coupled to a hollow fiber membrane filtration module (5×10^5 MW cutoff, GE). The AnMBR was fed with cheese whey obtained by diluting the powdered cheese whey in water, and operated under an organic loading rate (OLR) of 15 g sugars L^{-1} d^{-1}, pH controlled at 5–6 (through the automatic addition of 4*M* NaOH), temperature 30–37°C, and hydraulic and sludge retention times (HRT and SRT) of 1 and 4 days, respectively. The fermented CW produced, with the following average composition: 53 ± 3% acetate, 19 ± 1% propionate, 17 ± 4% butyrate, and 11 ± 1% valerate (% Cmol basis), was kept refrigerated at 4°C for short-time storage, 1 to 5 days, and frozen at −20°C for long-time storage. PHA accumulating mixed microbial culture selection was carried out in a 100 L stainless steel sequencing batch reactor (SBR). The SBR was fed with a synthetic organic acids mixture mimicking the fermented CW (50% acetate, 20% propionate, 20% butyrate, and 10% valerate, on % Cmol basis) supplemented with nutrients (NH_4Cl and KH_2PO_4, at a C/N/P ratio of 100/10/1), and operated at a feast and famine regime in 12 h cycles (four discrete phases: influent filling – 15 min; aeration – 680 min; settling – 30 min; and withdrawal of the exhausted effluent – 10 min), an OLR of 2.4 g HOrg L^{-1} d^{-1}, HRT of 1 day, and SRT of 4 days. The biomass purged from the selection reactor was used as inoculum for the PHA production assays. PHA production was carried out in a 20 L fed-batch reactor inoculated with c.a. 12.5 L of concentrated SBR biomass. The reactor was fed in a pulse-wise manner with the fermented CW, controlled by the dissolved oxygen (DO) response. When DO increased, a new pulse of fermented cheese whey was injected. This procedure was repeated until no DO response was observed. The pH of the fermented CW was previously adjusted to 6, with the addition of 5*M* NaOH.

A PHA cell content of ca. 30% (wt %) was attained. In order to recover the polymer, a quenching step (by adding 2*M* HCl) was performed directly on the mixed liquor, followed by a 3 h reaction with NaClO (1% Cl_2) in order to degrade the cellular material, then the polymeric material was recovered by centrifugation (20 min × 6500 rpm), washed once with distilled water, and dried in two temperature steps: 60°C for 2 days and 70°C 5 h. No further purification steps were followed to eliminate cell debris or other organic material from the polymer.

The PHBV blends were obtained by mixing different amounts of the u-PHBV with pellets of a commercial PHBV (Tianan Biopolymer, Ningbo, China) with 3 wt % valerate content (PHBV3) in a Brabender Plastograph mixer (Brabender, Germany) during 5 min at 100 rpm and at 175°C. The batches were subsequently compression molded into films using a hot-plate hydraulic press (Carver 4122, USA) at 175°C, 2 MPa and 4 min to produce films with a thickness of ∼200 μm.

Characterization of the u-PHBV

In order to ascertain the purity of the produced u-PHBV and compare its contents on Hydroxybutyrate (HB) and hydroxyvalerate (HV) to that of commercial PHBV, the lyophilized polymer powder was dissolved in chloroform (50 mL per gram of lyophilized powder) at 37°C for at least 2 days. The solution was then filtered to remove all non-$CHCl_3$ dissolved material, and the filtrate was used to fill glass Petri dishes. Finally, chloroform was evaporated, allowing polymer recovery in the form of a thin film. The contents on HB and HV was determined by gas chromatography (GC) using a method adapted from Serafim *et al.*[3] Briefly, lyophilized biomass was incubated for methanolysis in a 20% sulfuric acid in methanol solution (1 mL) and extracted with chloroform (1 mL). The mixture was digested at 100°C for 3.5 h. After the digestion step, the methylated monomers were extracted and injected (2 μL) into a gas chromatograph equipped with a flame ionization detector (Bruker 430-

GC) and a BR-SWax column (60 m, 0.53 mm internal diameter, 1 μm film thickness, Bruker, USA), using helium as carrier gas at 1.0 mL/min. Samples were analyzed under a temperature regime starting at 40°C, increasing to 100°C at a rate of 20°C/min, to 175°C at a rate of 3°C/min, and reaching a final temperature of 220°C at a rate of 20°C/min for ensuring cleaning of the column after each injection. Injector and detector temperatures were 280°C and 230°C, respectively. HV and HB concentrations were determined using two calibration curves, one for HB and other for HV, using standards (0.1–10 g L^{-1}) of a commercial P(HB-HV) (88%/12%) (Sigma), and corrected using heptadecane as internal standard (concentration of approximately 1 g L^{-1}). Average molecular weights were determined using a size exclusion chromatography (SEC) apparatus (Waters) as described by Serafim *et al.*[12] The protein content was determined by the Lowry protein assay with bovine serum albumin as calibrant.

Characterization of the PHBV Blends

Scanning Electron Microscopy (SEM) of all the samples was conducted using a high resolution field-emission JEOL 7001F. The samples were fractured in liquid nitrogen and then were coated by sputtering with a thin layer of Pt prior to SEM observation. Energy dispersive system (EDS) analysis was performed to obtain local chemical information.

Thermal stability of the nanocomposites was investigated by means of thermogravimetric analyses (TGA) using a TG-STDA Mettler Toledo model TGA/SDTA851e/LF/1600. The samples were heated from 50°C to 900°C at a heating rate of 10°C/min under nitrogen flow.

Differential scanning calorimeter experiments were conducted using a Perkin-Elmer DSC-7. The weight of the DSC samples was around 6–8 mg. Samples were first heated from 45°C to 200°C at 40°C/min, kept for 1 min at 200°C, cooled down to 45°C at 10°C/min, and then heated to 200°C at 10°C/min. The crystallization temperature (Tc), crystallization enthalpy (ΔHc), melt temperature (Tm), and melting enthalpy (ΔHm) were determined from the cooling and second heating curve. Tm and ΔHm were taken as the peak temperature and the area of the melting endotherm, respectively. The crystallinity (Xc) of the PHBV phase was calculated by the following expression:

$$X_c(\%) = \frac{\Delta H_m}{w \cdot \Delta H_m^0} \times 100$$

where ΔHm (J/g) is the melting enthalpy of the polymer matrix, (ΔH0m) is the melting enthalpy of 100% crystalline PHBV (perfect crystal) (146 J/g), and w the weight of the PHBV fraction in the blend, considering a 70% purity of the u-PHBV.[13] The DSC instrument was calibrated with an indium standard before use.

Tensile properties were measured in a universal testing machine (Instron 4469) at a crosshead speed of 10 mm/min and room temperature. Tests were made according to ASTM D638 using films of approximately 100-μm thickness prepared by hot press. Five specimens of each sample were tested and the average results with standard deviation were reported.

Blend samples were compression molded (at 180°C, 20 tons for 3 min) into 1mm thick disks of 40 mm diameter. Disks were loaded between the parallel plates of a stress controlled rheometer (ARG2, TA Instruments) preheated at 180°C. A time sweep tests with strain of 1% applied at 1 Hz was first performed during 5 min. Finally, the temperature was dropped to 160°C and the time dependence of both storage (G′) and loss (G″) moduli were recorded at 1 Hz and for a strain of 1%, as for assessing the crystallization kinetics at this temperature. Note here that mechanical spectra of unpurified PHBV could not be recorded due to the very fast thermal degradation leading to a dramatic drop in viscosity with time, which could not be corrected for in the mechanical spectrum.

The water vapor permeability (WVP) of the PHBV blends was measured according to the ASTM E96 (2011) gravimetric method, using Payne permeability cups (Elcometer, Hermelle Argenteau, Belgium). Distilled water was placed inside the cup to expose the film (the exposed area was 9.6×10^{-4} m^2) to 100% RH on one side. Once the films were secured, each cup was placed in an equilibrated relative humidity dessicator at 24°C. Relative humidity at 0% was held constant using silica gel. The cups were weighed periodically (± 0.0001 g), at least twice a day for 7 days. Aluminum foil was used as a control to rule out vapor loss through the sealing. WVP was calculated from the steady-state permeation slopes obtained from the regression analysis of weight loss data over time. The permeability to D-Limonene (Panreac, Barcelona, Spain) was measured analogously, filling the cups with the volatile compound instead of distilled water. The lower limit of vapor permeability detection of the permeation cells was of $\sim 1 \cdot 10^{-17}$ and $5 \cdot 10^{-17}$ kg m/s m^2 Pa for water vapor and D-Limonene, respectively, based on the weight loss measurements through the sealing in aluminum samples. All measurements were performed in triplicate.

RESULTS AND DISCUSSION

Characterization of the u-PHBV

It is well known that the properties of PHAs are drastically affected by their valerate content, this endowing higher flexibility, elongation at break, and a lower melting temperature to the PHA. Therefore, it was essential to determine the purity and HB : HV composition of u-PHBV in order to compare it with the commercial PHBV used in this study. A typical GC chromatogram of the monomer profiles of u-PHBV is shown in Figure 1. Three main peaks can be observed, which can be ascribed to the derivatives of hydroxybutyrate, hydroxyvalerate, and the internal standard, heptadecane, respectively. A summary of the calculated characteristics of both PHAs used in this study is presented in Table I. Impurities can be mainly ascribed to proteins although small quantities of sugars and water (<0.5%) were detected (data not shown). The results on the characterization of u-PHBV are in agreement with previous works at the same conditions,[11] which further stresses the possibility of reproducibly tuning the PHA composition by adjusting the fermentation process. Nevertheless, it must be noted that lower accumulation yields of PHA were achieved in this larger scale work, as compared to the previous study. This was probably

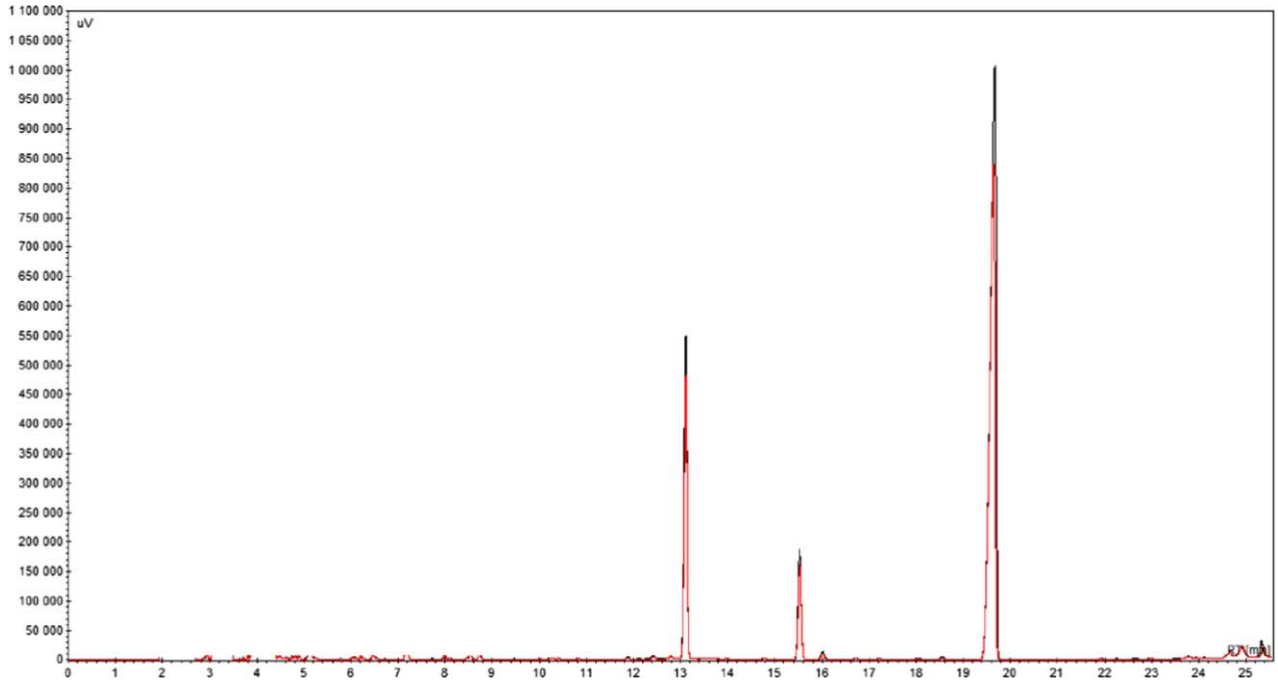

Figure 1. GC chromatogram of u-PHBV (red line), hydroxybutyrate and hydroxyvalerate standards (black line) after acid methanolysis. Heptadecane was used as internal standard. [Color figure can be viewed in the online issue, which is available at wileyonlinelibrary.com.]

due to lower oxygen transfer efficiency, which evidences the opportunity for further optimization of the larger scale process.

Characterization of the PHBV Blends

Morphology. Figure 2 shows representative scanning electron micrographs of the cryofractured surface of the samples without and with 7 wt % and 20 wt %, respectively. The presence of impurities can be observed in all the samples, this being more evident in samples with higher u-PHBV contents. The impurities are tightly bonded to the polymer as derived from the coherent interface, thus revealing a good degree of interaction. EDS spot experiments were conducted on these impurities in order to determine the chemical elements present. An organic (C, O, H) nature was revealed, which may be ascribed to remnants of small amounts of cell debris or fatty acids from the production process.

Thermal Stability. The effect of the addition of u-PHBV to neat PHBV on the thermal stability of PHBV was assessed by means of TGA and rheometry. Thermogravimetric analyses were carried out to investigate the effect of the non-purified PHBV on the thermal stability and degradation behavior of PHBV blends. Figure 3(a) shows the mass loss vs. temperature curves for all the systems studied. From this plot, it can be stated that full degradation of the organic part of the sample takes place at temperatures between 260 and 310°C. Moreover, no significant mass was lost in any of the samples before the main degradation step took place. The remnant mass after polymer degradation is attributed to the boron nitride used as nucleating agent in the commercial PHBV grade.

Figure 3(b) presents an amplification of the DTG curve for the degradation event. According to the literature,[14] PHBV thermodegradation takes place by a random chain scission mechanism in a single step between 260 and 300°C. The addition of unpurified PHBV resulted in a slight shift of the maximum rate towards lower temperature values. Additionally, the temperature at which degradation starts was also slightly decreased. However, this effect does not seem to be affected by the amount of incorporated u-PHBV, which indicates that the presence of the organic/non polymeric impurities or metal ions within the unpurified PHBV might be catalyzing its degradation to a certain extent. Nevertheless, this slight decrease in the onset of degradation and degradation rates may not be sufficient as to affect the thermal processability of these materials in practical terms.

Rheometry was carried out to further assess the influence of u-PHBV on the stability of the blends. Figure 4 shows that the time dependence of the dynamic viscosity recorded during 5

Table I. Comparative Characterization of the Unpurified PHBV Obtained from Mixed Bacterial Cultures (u-PHBV) and the Commercial PHBV Used in This Study

Sample	u-PHBV	Commercial PHBV
Purity (%)	90	n.c.[a]
HB : HV contents (%)	81.7 : 18.3	95 : 5
Protein contents (%)	5.3	n.c.
Ashes (%)	3.0	n.c.
Molecular weight (D)	3.6×10^5	3.8×10^5
Polydispersity index	1.7	1.6

[a] n.c.: not calculated.

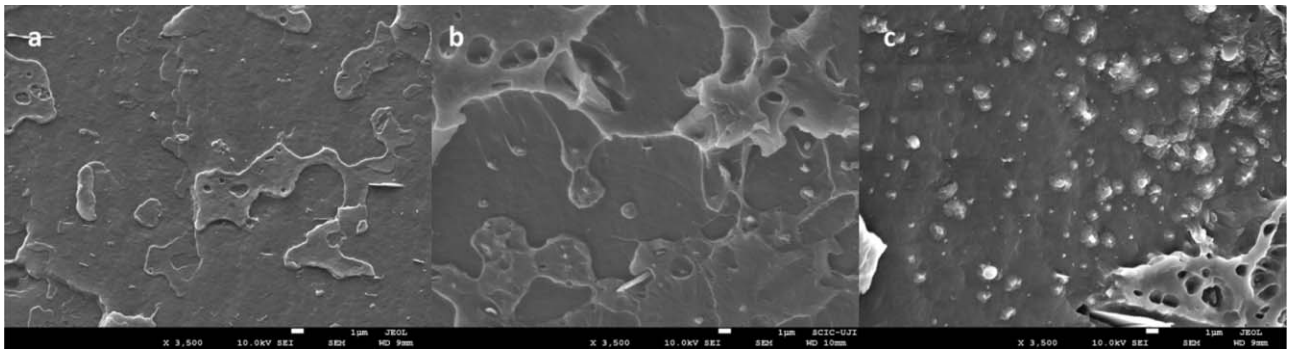

Figure 2. SEM micrographs of neat PHBV (a) and PHBV blend incorporating 7 wt % (b) and 20 wt % (c) u-PHBV.

min at 180°C is significantly weaker when only 5 wt % unpurified PHBV is added compared to the commercial PHBV. Indeed, for 20 wt % the viscosity is nearly constant after 5 min. This suggests that the chain scission, which drives the viscosity drop as the result of the thermally accelerated PHBV degradation is less important when unpurified PHBV is added. The latter may therefore act as a viscosity stabilizer against thermal degradation. However, the stabilizing effect comes at the cost of a decreased viscosity, since the blend with 20 wt % unpurified PHBV shows a nearly 20 times smaller viscosity when compared with the neat commercial PHBV.

Crystallization. Both the crystallinity of the blends and their crystallization behavior were investigated by means of DSC and rheometry, respectively. As can be seen in Table II, there is a gradual drop in both crystallization and melting temperatures with increased u-PHBV incorporated into the melt. This point towards a crystallite population of decreasing size or decreased lamellar thickness. However, at higher u-PHBV contents, two separate melting enthalpies denoted the presence of an additional crystallite population with the same thermal characteristics as the reference sample [Figure 5(a)]. This second melting might however be the result of a melting-recrystallization process, as previously reported for this type of polymers.[15,16] The crystalline fraction, as calculated from the melting enthalpies of the blends, is also shown to slightly decrease with increasing u-PHBV contents. Nevertheless, notable differences are only observed with contents higher than 10 wt % of incorporated u-PHBV. This indicates the crystalline fraction is not considerably affected by the incorporation of small quantities of u-PHBV. As far as the crystallization is concerned, in the DSC cooling runs a slight shift to lower crystallization temperatures of the blends is observed with increasing uPHBV contents [Figure 5(b)]. This could be explained by reduced concentration of the nucleating agents (included in the commercial PHBV) as well as by the increase in impurities in the polymer melts. This effect was also investigated by means of rheometry analysis. The isothermal crystallization kinetics of the blends at 160°C was studied by following the time evolution of the elastic storage moduli G'. In Figure 6, the crystallization behavior of blends without and

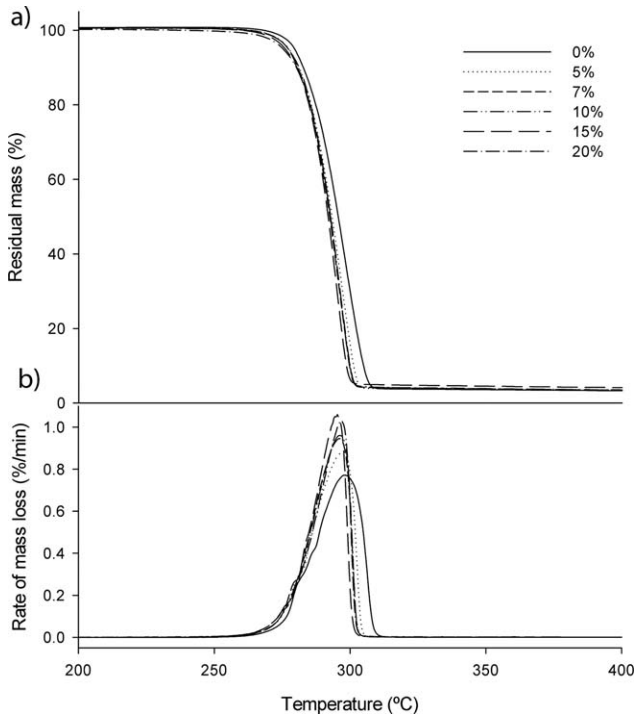

Figure 3. Thermogravimetric analysis displaying mass loss (a) and rate of mass loss (b) of the PHBV blends with increasing u-PHBV contents.

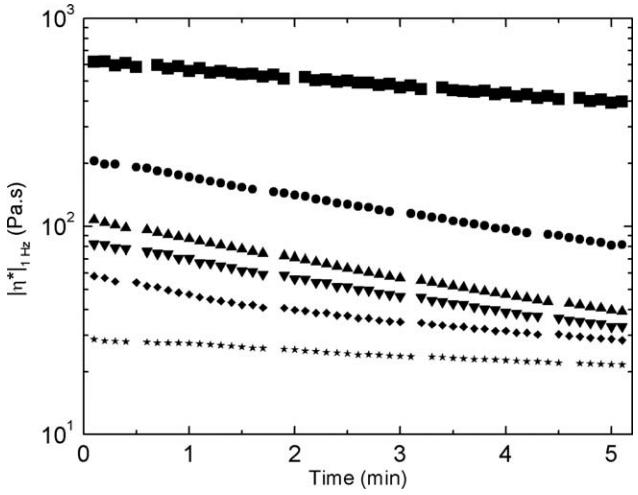

Figure 4. Time dependence of the dynamic viscosity recorded at 1 Hz, $|\eta^*|_{1\ Hz}$ just after loading samples disks in the rheometer at 180°C: neat commercial PHBV (squares) blended with 5 wt % (circles), 7 wt % (up triangles), 10 wt % (down triangles), 15 wt % (diamonds), and 20 wt % (stars) unpurified PHBV.

Table II. Thermal Properties of the PHBV Blends

u-PHBV content (%)	T_c	ΔH_c	T_{m1}	T_{m2}	ΔH_m	X_c (%)[a]
0%	114.6±0.8	85.4±0.6	172.3±0.6	-	94.0±0.6	64.4±0.4
5%	113.2±0.1	83.4±1.2	171.0±0.2	-	92.2±0.6	63.5±0.4
7%	109.6±0.1	80.4±0.9	169.5±0.2	-	90.1±1.8	62.1±1.2
10%	107.2±0.2	79.4±0.6	168.8±0.1	172.0±0.3	89.4±2.2	61.9±1.0
15%	106.5±1.2	76.8±0.5	167.8±0.4	172.3±0.1	86.9±1.5	60.4±1.0
20%	103.3±0.7	73.6±1.5	164.8±1.3	172.4±0.4	84.3±0.1	58.9±0.1

[a] For the calculation of crystallinity (X_c), only the chloroform extractable fraction of u-PHBV was considered.

with the maximum added contents of u-PHBV are presented. At early times, scattering in G' data originating from the cooling from 180°C and the thermal equilibration at 160°C (see right axis where the time dependences of samples temperatures are reported) impedes capturing the onset of crystallization. Although there is a slight delay in isothermal crystallization with the addition of u-PHBV, full crystallinity was achieved in all cases after 2000 sec. The slight delay at early stages may be explained by decreased concentration of nucleating agents carried by the commercial PHBV.

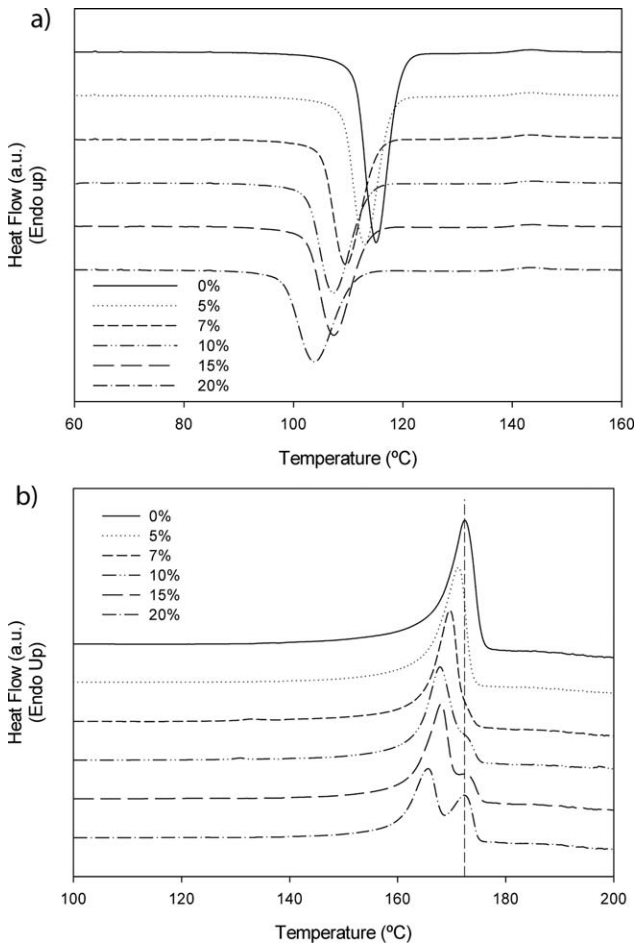

Figure 5. DSC thermograms of heating (a) and cooling runs (b) at 10°C/min of PHBV blends with increasing u-PHBV content.

Mechanical Properties. Mechanical properties of the PHBV blends were assessed by tensile tests. Figure 7 gathers the results obtained from the strain stress curves of the PHBV blends as a function of u-PHBV contents. It can be observed that the addition of u-PHBV leads to a decrease in the Young's modulus of the PHBV, this effect being higher with increasing u-PHBV contents (e.g. The sample containing a 20% of uPHBV presents a decrease in the stiffness of the material of ca. 25%). This decrease tendency in the elastic modulus of the materials correlates with a subsequent decrease in the stress at break, e.g. around 30% decrease in blends with 20 wt % u-PHBV contents, which is indicating that the unpurified PHBV has a plasticizing effect on the raw PHBV. Furthermore, the elongation at break of the PHBV blends is found to slightly increase with the addition of unpurified PHBV, reaching a maximum of 3.15 for samples with 15 wt %, thus confirming the plasticizing effect. All these changes can be attributed to increasing contents of HV in the PHBV, as in line with results for similar HV contents in PHBV.[4] However, the contribution of the present impurities (fatty acids, proteins or further cell debris) to these changes cannot be ruled out and may be further addressed in the future. Samples containing larger amounts of u-PHBV suffered a drop in the strain at break (εR), possibly attributed to the presence of a high concentration of these non-polymeric impurities (as detected by SEM) that could act as stress concentrators.

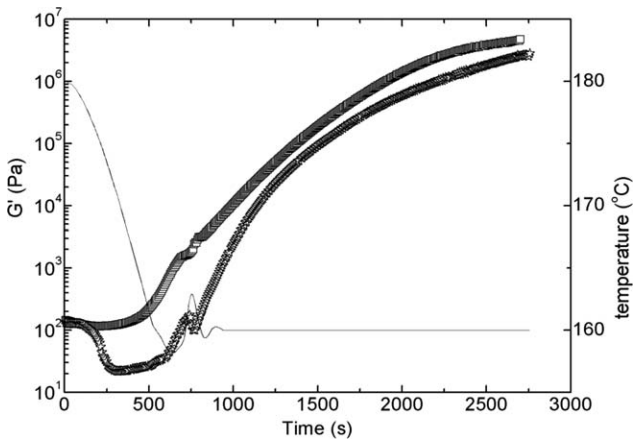

Figure 6. Crystallization kinetics at 160°C of commercial PHBV and blends with 20 wt % unpurified PHBV. Symbols are as in Figure 4. The thin solid line reports the temperature-time dependances of reported samples (see right axis).

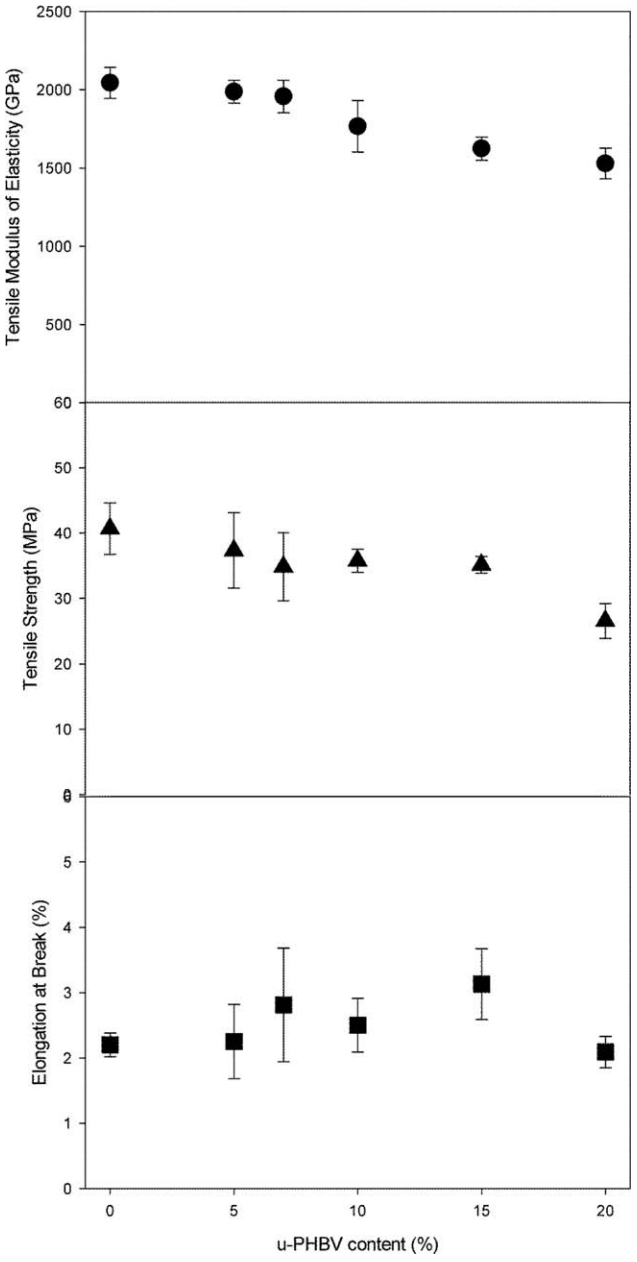

Figure 7. Tensile properties of PHBV blend with increasing u-PHBV.

Permeability Measurements. Water vapor permeability by weight loss or gain measurements (ASTM E96) are common methods to determine the water barrier properties of materials, while D-Limonene is a commonly used standard compound to test mass transport of volatile compounds, such as aromas. Figure 8 shows the vapor permeability values of blends with increasing u-PHBV contents for the two compounds. Values for both water and D-limonene vapor permeability of blends with up to 15 wt % u-PHBV are not substantially affected. A very slight increase in water vapor permeability can be noted in this range of incorporated u-PHBV, which may nevertheless not be significant. In general terms, permeability values are relatively low (close to the detection limit of the technique) and quite similar regardless of the incorporation of u-PHBV, the deviations oscillating between 5×10^{-17} and 5×10^{-16} kg/m Pa s. Only PHBV blends with the highest u-PHBV contents (20 wt %) display a decrease in the water and aroma barrier properties, which is still within the same order of magnitude. This decrease may be attributed to the possible combination of decreased crystallinity, plasticization, or the presence of defects and discontinuities within the polymer structure due to higher contents of the heterogeneous u-PHBV. These results point out that the incorporation of relatively high quantities of the u-PHBV does not drastically affect the barrier properties of the materials against water or aroma compounds.

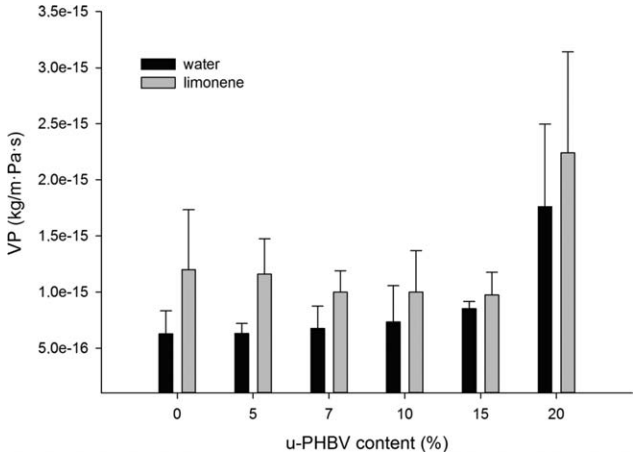

Figure 8. Vapor Permeability measurements of PHBV blends with increasing u-PHBV to water vapor and limonene.

CONCLUSION

PHBV was produced in a pilot plant scale from mixed microbial cultures and using a cheese whey industrial by-product according to optimization protocols reported in a previous study. The characterization of the u-PHBV revealed a good reproducibility for a potential upscaling. The u-PHBV was incorporated without previous purification or isolation processes into commercial PHBV. Although the presence of different impurities from the fermentation stages was evident, these did not substantially affect the crystallinity or the thermal, mechanical or barrier properties of the polymer fraction of the materials for loadings of up to 10 wt % u-PHBV. The detrimental effect with higher loadings poses new challenges as to optimization of the PHA production or the use of other polymeric matrices for the blends. Nevertheless, the absence of purification steps, the valorization of industrial waste by-products as well as the relative preservation of physicochemical properties when incorporated in the blends supports the use of this PHBV in its unpurified form to derive more cost effective PHA based products such as packaging articles.

ACKNOWLEDGMENTS

The authors acknowledge financial support from the Spanish MINECO (MAT2012-38947-C02-01 project) and from the European FP7 ECOBIOCAP project. The work was also partially supported by FEDER funds through the program COMPETE (project PTDC/AGR-ALI/122741/2010) by the Portuguese Foundation for

Science and Technology (PEst-C/CTM/LA0025/2013 – Projecto Estratégico – LA 25 – 2013–2014– Strategic Project – LA 25 – 2013–2014) and by Programa Operacional Regional do Norte (ON.2) through the project "Matepro –Optimizing Materials and Processes", with reference NORTE-07-0124-FEDER-000037 FEDER COMPETE.

REFERENCES

1. Rehm, B. H. A. *Biochem. J.* **2003**, *376*, 15.
2. Reis, M. A. M.; Serafim, L. S.; Lemos, P. C.; Ramos, A. M.; Aguiar, F. R.; Van Loosdrecht, M. C. M. *Bioprocess Biosystems Eng.* **2003**, *25*, 377.
3. Serafim, L. S.; Lemos, P. C.; Oliveira, R.; Reis, M. A. M. *Biotechnol. Bioeng.* **2004**, *87*, 145.
4. Laycock, B.; Halley, P.; Pratt, S.; Werker, A.; Lant, P. *Prog. Polym. Sci.* **2013**, *38*, 536.
5. Khanna, S.; Srivastava, A. K. *Process Biochem.* **2005**, *40*, 607.
6. Keshavarz, T.; Roy, I. *Curr. Opin. Microbiol.* **2010**, *13*, 321.
7. Nduko, J. M.; Matsumoto, K.; Taguchi, S. In ACS Symp. Series, **2012**, American Chemical Society, Wahington DC, USA, p 213.
8. Jacquel, N.; Lo, C.-W; Wei, Y.-H; Wu, H.-S; Wang, S.-S. *Biochem. Eng. J.* **2008**, *39*, 15.
9. Albuquerque, M. G. E.; Torres, C. A. V.; Reis, M. A. M. *Water Res.* **2010**, *44*, 3419.
10. Gurieff, N.; Lant, P. *Bioresour. Technol.* **2007**, *98*, 3393.
11. Duque, A. F.; Oliveira, C. S. S.; Carmo, I. T. D.; Gouveia, A. R.; Pardelha, F.; Ramos, A. M.; Reis, M. A. M. *N. Biotechnol.* **2014**, *31*, 276.
12. Serafim, L. S.; Lemos, P. C.; Torres, C.; Reis, M. A. M.; Ramos, A. M. *Macromol. Biosci.* **2008**, *8*, 355.
13. Liu, Q.-S.; Zhu, M.-F; Wu, W.-H; Qin, Z.-Y. *Polym. Degrad. Stab.* **2009**, *94*, 18.
14. Grassie, N.; Murray, E. J.; Holmes, P. A. *Polym. Degrad. Stab.* **1984**, *6*, 127.
15. Gunaratne, L. M. W. K.; Shanks, R. A. *Eur. Polym. J.* **2005**, *41*, 2980.
16. Barham, P. J.; Keller, A.; Otun, E. L.; Holmes, P. A. *J Mat Sci,* **1984**, *19*, 2781.